

INL REPORT

INL/EXT-16-39930

Unlimited Release

Printed September 2016

Initial Testing of the Microscopic Depletion Implementation in the MAMMOTH Reactor Physics Application

Javier Ortensi, Sebastian Schunert, Yaqi Wang, Barry D. Ganapol, Frederick N. Gleicher,
Benjamin A. Baker and Mark D. DeHart

Prepared by
Idaho National Laboratory
Idaho Falls, Idaho 83415

The Idaho National Laboratory is a multiprogram laboratory operated by
Battelle Energy Alliance for the United States Department of Energy
under DOE Idaho Operations Office. Contract DE-AC07-05ID14517.

Approved for public release; further dissemination unlimited.



Issued by the Idaho National Laboratory, operated for the United States Department of Energy by Battelle Energy Alliance.

NOTICE: This report was prepared as an account of work sponsored by an agency of the United States Government. Neither the United States Government, nor any agency thereof, nor any of their employees, nor any of their contractors, subcontractors, or their employees, make any warranty, express or implied, or assume any legal liability or responsibility for the accuracy, completeness, or usefulness of any information, apparatus, product, or process disclosed, or represent that its use would not infringe privately owned rights. Reference herein to any specific commercial product, process, or service by trade name, trademark, manufacturer, or otherwise, does not necessarily constitute or imply its endorsement, recommendation, or favoring by the United States Government, any agency thereof, or any of their contractors or subcontractors. The views and opinions expressed herein do not necessarily state or reflect those of the United States Government, any agency thereof, or any of their contractors.



INL/EXT-16-39930
Unlimited Release
Printed September 2016

Initial Testing of the Microscopic Depletion Implementation in the MAMMOTH Reactor Physics Application

Javier Ortensi¹, Sebastian Schunert², Yaqi Wang²,
Barry D. Ganapol³, Fredrick N. Gleicher¹, Benjamin A. Baker¹ and Mark D. DeHart¹

¹Reactor Physics Design and Analysis Department
Idaho National Laboratory
P.O. Box 1625
Idaho Falls, ID 83415-3840

²Nuclear Engineering Methods and Development Department
Idaho National Laboratory
P.O. Box 1625
Idaho Falls, ID 83415-3840

³Department of Aerospace and Mechanical Engineering
University of Arizona
1209 East 2nd Street, Room 100
Tucson, Arizona 85721

Abstract

Present and new nuclear fuels that will be tested at the Transient Reactor Test (TREAT) facility will be analyzed with the MAMMOTH reactor physics application, currently under development, at Idaho National Laboratory. MAMMOTH natively couples the BISON, RELAP-7, and Rattlesnake applications within the MOOSE framework. This system allows the irradiation of fuel from beginning of life in a nuclear reactor until it is placed in TREAT for fuel testing within the same analysis mesh and, thus, retaining a very high level of resolution and fidelity. The calculation of the isotopic distribution in fuel requires the solution to the decay and transmutation equations coupled to the neutron transport equation. The Chebyshev Rational Approximation Method (CRAM) is the current state-of-the-art in the field, as was chosen to be the solver for the decay and transmutation equations. This report shows that the implementation of the CRAM solver within MAMMOTH is correct with various analytic benchmarks for decay and transmutation of nuclides. The results indicate that the solutions with CRAM order 16 achieve the level of precision of the benchmark. The CRAM solutions show little sensitivity to the time step size and consistently produce a high level of accuracy for isotopic decay for time steps of 1×10^{11} years. Comparisons to DRAGON5 with 297 isotopes yield comparable results, but some differences need to be further analyzed.

Acknowledgments

We would like to acknowledge Derek Lax for his contribution in the initial implementation of the CRAM solver. The Authors are also grateful for Alain Hebert's support with the DRAGON5 calculations. This work was performed under funding provided by the U.S. Department of Energy's Nuclear Energy Advanced Modeling and Simulation program.

Contents

1	Introduction	1
2	Theory	3
2.1	Decay and Transmutation Equations	3
2.2	The Chebyshev Rational Approximation Method	4
2.3	Consistency of the Chebychev Rational Approximation Method	6
3	Test Problems	9
3.1	Thorium Series	9
3.2	Constant Flux in a Homogeneous System	10
3.3	Code-to-Code Comparison to DRAGON5	10
4	Results	13
4.1	Thorium Series	13
4.2	Constant Flux in a Homogeneous System	16
4.3	Code-to-Code Comparison to DRAGON5	19
5	Conclusions and Future Work	27
	References	29

Figures

1	Thorium-232 decay series.....	10
2	Irradiation history for constant flux test.	11
3	CRAM order convergence for the Thorium chain.	13
4	Relative error of the MAMMOTH Thorium chain solution at 1 year. (Benchmark accuracy $\sim 1 \times 10^{-12}$ relative error)	14
5	Relative error of the MAMMOTH Thorium chain solution at 100 billion years. (Benchmark accuracy $\sim 1 \times 10^{-9}$ relative error)	15
6	Reference and MAMMOTH solution for the Xe-135 chain.	16
7	CRAM order convergence for the Xe-135 chain (1 hr time step). (Benchmark accuracy $\sim 1 \times 10^{-12}$ relative error)	17
8	Relative error for the Xe-135 chain with large time steps. (Benchmark accuracy $\sim 1 \times 10^{-12}$ relative error)	18
9	Reactivity curve for the homogeneous infinite domain problem.	20
10	Isotopic concentrations and relative differences for U235.	21
11	Isotopic concentrations and relative differences for Pu239.	22
12	Isotopic concentrations and relative differences for Pu240.	23
13	Isotopic concentrations and relative differences for I135.	24
14	Isotopic concentrations and relative differences for XE135.	25
15	Isotopic concentrations and relative differences for SM149.	26

Tables

1	Relative difference between right and left hand side of the conditions layed out in Eq. 22 for different CRAM orders.	7
2	Decay constants for the Thorium Series (per day).....	9
3	Branching ratios for Bi-212	10
4	Reference solution for Thorium Series at 1 year. (1×10^{-12} relative error)	11

1 Introduction

Current and new nuclear fuels will be tested at the Transient Reactor Test (TREAT) facility. Some of these will be fresh fuel samples and other will be irradiated. The accurate modeling of irradiated nuclear fuel necessitates knowledge of the local power, flux and isotopic distribution during the irradiation time.

Idaho National Laboratory plans to use MAMMOTH [1] for the analysis of TREAT experiments in order to achieve high fidelity in the modeling of nuclear fuel. MAMMOTH is the MOOSE-based [2] reactor physics application that natively couples the fuel performance code BISON [3], the thermal fluids code RELAP-7 [4] and the neutron transport code Rattlesnake [5]. Some of this capability has been tested with the macroscopic depletion in MAMMOTH for a full size LWR pin followed with a Station Black Out (SBO) accident condition [6]. MAMMOTH will allow the irradiation of fuel from beginning of life in a nuclear reactor until it is placed in TREAT for fuel testing using the same analysis mesh and, thus, retaining a very high level of resolution and fidelity.

The calculation of the isotopic distribution in fuel requires the solution to the decay and transmutation equations coupled to the neutron transport equation. The Chebyshev Rational Approximation Method (CRAM) is the current state-of-the-art in the field, and is chosen due to its stability for solving the equations with many isotopes and large time steps. This work documents the initial testing of the CRAM implementation in the MAMMOTH application.

2 Theory

2.1 Decay and Transmutation Equations

The equation that describes the time rate of change of the i^{th} nuclide in a material due to nuclear decay is known as the Bateman Equation [7] and is formulated as:

$$\frac{dN_i}{dt} = \sum_{j=1}^J \lambda_j N_j(t) \beta_{j \rightarrow i} - \lambda_i N_i(t), \quad (1)$$

where

J is the number of parent nuclides that produce the i^{th} nuclide

N_i is the concentration of the i^{th} nuclide,

λ_j is the decay constant of the j^{th} parent nuclide,

λ_i is the decay constant of the i^{th} nuclide,

$\beta_{j \rightarrow i}$ is the decay branching ratio (probability that a decay of the j^{th} nuclide leads to production of the i^{th} nuclide)

In a transmutation environment (i.e. a neutron flux in a nuclear reactor) the time rate of change of the nuclide can be affected by other processes that can lead to the production and/or destruction of the i^{th} nuclide

$$\frac{dN_i}{dt} = \sum_{j=1}^J (\lambda_j \beta_{j \rightarrow i} + \sum_{g=1}^G \sigma(t)_{n,j}^g \phi(t)^g \alpha_{j \rightarrow i}^g) N_j(t) - (\lambda_i + \sum_{g=1}^G \sigma(t)_{a,i}^g \phi(t)^g) N_i(t), \quad (2)$$

where

$\sigma_{n,j}^g$ is the microscopic cross section for an interaction of type n for the j^{th} nuclide in group g

ϕ^g is the flux in group g

$\alpha_{j \rightarrow i}^g$ is the reaction branching ratio from the j^{th} to the i^{th} nuclide in group g

$\sigma_{a,i}^g$ is the microscopic absorption cross section for the i^{th} nuclide in group g

The problem can be formulated as a system of coupled ordinary differential equations with a properly defined initial condition,

$$\frac{d\vec{N}}{dt} = \mathbf{A}(t)\vec{N}, \quad (3)$$

$$\vec{N}(0) = \vec{N}_0$$

where

\vec{N} is the vector formed by all isotope densities, and i is then the index in this vector for the isotope N_i .

The matrix coefficients take the form

$$A_{i,j} = -\lambda_i^{eff} \delta_{ij} + b_{i,j}^{eff}, \quad (4)$$

where (δ_{ij}) is the Kronecker delta function and the effective decay/destruction coefficient, λ_i^{eff} , populates the main diagonal of the matrix

$$\lambda_i^{eff} = \lambda_i + \sum_{g=1}^G \sigma_{a,i}^g \phi^g, \quad (5)$$

and the effective decay/transmutation coefficient, $b_{i,j}^{eff}$, populates the off-diagonal terms

$$b_{i,j}^{eff} = \lambda_j \beta_{j \rightarrow i} + \sum_{g=1}^G \sigma_{n,j}^g \phi^g \alpha_{j \rightarrow i}^g. \quad (6)$$

2.2 The Chebyshev Rational Approximation Method

The solution to the system of ODEs defined in Equation 3 varies in level of complexity and it is mainly driven by the time scales (magnitude of the coefficients) in the matrix. For the majority of applications, the system is stiff leading to instabilities in explicit methods with large time steps. In addition, implicit methods are slow and inaccurate. Therefore, matrix exponential and linear chains methods are the typical choices. The matrix exponential form of the solution assuming constant a constant flux is

$$\vec{N}(t) = e^{At} \vec{N}_0, \quad (7)$$

where the matrix exponential, e^{At} , is defined by the power series

$$e^{At} = \sum_{k=0}^{\infty} \frac{1}{k!} (At)^k, \quad (8)$$

with the required definition

$$\mathbf{A}^0 = \mathbf{I}. \quad (9)$$

Typically, the matrix exponential is solved via a truncated Taylor series or a rational Padé approximation. However, these solutions rely on a small value of the matrix norm $\|\mathbf{A}t\|$. Due to the nature of the burnup equations, this norm can reach values greater than 10^{20} , causing significant numerical inaccuracies. The introduction of the Chebyshev Rational Approximation Method (CRAM) [8] method was based on the observation that the eigenvalues were mostly clustered close to the negative real axis in the burnup matrix. CRAM has been shown to currently be the most accurate and computationally efficient method for solving the matrix exponential given this constraint on the eigenvalues. The matrix exponential is computed from a rational function $r(z)$ that is known to be a good approximation to the function e^z in some region in the complex plane \mathbb{C} .

Introducing the rational approximation for the matrix exponential leads to

$$\vec{N}(t) = e^{\mathbf{A}t} \vec{N}_0 \approx r_{k,k}(-\mathbf{A}t) \vec{N}_0, \quad (10)$$

where $r_{k,k}(-\mathbf{A}t)$ is the rational approximation.

If a rational approximation

$$r_{k,k}(z) = \frac{p_k(z)}{q_k(z)}, \quad (11)$$

has simple poles and p_k and q_k are functions of polynomial of order k , the partial fraction decomposition (PFD) takes the form

$$r_{k,k}(z) = \alpha_0 + \sum_{j=1}^k \frac{\alpha_j}{z - \theta_j}. \quad (12)$$

where

- α_0 = limit of the function $r_{k,k}$ at infinity
- α_j = residues at the poles θ_j .

Since the poles of the rational function with real valued coefficients form conjugate pairs, the problem can be solved with half the number of computations

$$r_{k,k}(z) = \alpha_0 + 2Re \left(\sum_{j=1}^{k/2} \frac{\alpha_j}{z - \theta_j} \right). \quad (13)$$

A second approach is obtained using incomplete partial fractions (IPF) [8] and takes the form

$$r_{k,k}(z) = \alpha_0 \prod_{l=1}^{k/2} \left\{ 1 + 2Re \left(\frac{\tilde{\alpha}_l}{z - \theta_l} \right) \right\} \quad (14)$$

where $\tilde{\alpha}_l$ are the residues of a separate factorization and are different from those employed in the PFD rational approximation.

The PFD form of the solution is, therefore,

$$\vec{N} = \alpha_0 \vec{N}_0 + 2Re \left(\sum_{j=1}^{k/2} \alpha_j (\mathbf{A}t - \theta_j \mathbf{I})^{-1} \vec{N}_0 \right) \quad (15)$$

and the IPF form of the solution is

$$\vec{N} = \alpha_0 \vec{N}_0 \prod_{l=1}^{k/2} \left\{ 1 + 2Re \left(\tilde{\alpha}_l (\mathbf{A}t - \theta_l \mathbf{I})^{-1} \right) \right\}. \quad (16)$$

Both methods result in a system of $k/2$ independent sparse linear systems, which means that there is an inherent parallel nature to CRAM, at least insofar as the $k/2$ linear systems are concerned. This work focuses on the testing of the PFD method, since some issues were encountered in the IPF publication [8]. The author of the original paper on IPF was contacted in order to resolve these issues. The great advantage of the IPF is that it is less sensitive to round-off errors due to the smaller number of vectors being added during the computation. Therefore, future work will include the corrected implementation and testing of the IPF method.

2.3 Consistency of the Chebychev Rational Approximation Method

The matrix exponential can be computed using a Taylor series expansion:

$$\exp(\underline{\underline{A}}t) = \sum_{k=0}^{\infty} \frac{1}{k!} (\underline{\underline{A}}t)^k, \quad (17)$$

but this form it is not suitable for a numerical evaluation of the matrix exponential. Nevertheless, one can use Eq. 17 to find that:

$$\exp(\underline{\underline{A}}t) = \underline{\underline{I}} + \underline{\underline{A}}t + \frac{1}{2} \underline{\underline{A}}^2 t^2 + O(t^3). \quad (18)$$

The inverse of a sum of matrices can be expanded in a power series as follows:

$$(\underline{\underline{P}} + \underline{\underline{Q}}\varepsilon) = \underline{\underline{P}}^{-1} - \varepsilon \underline{\underline{P}}^{-1} \underline{\underline{Q}} \underline{\underline{P}}^{-1} + \varepsilon^2 \underline{\underline{P}}^{-1} \underline{\underline{Q}} \underline{\underline{P}}^{-1} \underline{\underline{Q}} \underline{\underline{P}}^{-1} + O(\varepsilon^3) \quad (19)$$

Using Eq. 19 in Eq. 13 leads to:

$$\left\{ \alpha_0 \underline{\underline{I}} + 2\text{Re} \left[\sum_{j=1}^{k/2} \alpha_j (\underline{\underline{A}}t - \theta_j \underline{\underline{I}})^{-1} \right] \right\} = \left\{ \alpha_0 \underline{\underline{I}} + 2\text{Re} \left[\sum_{j=1}^{k/2} \left(-\frac{\alpha_j}{\theta_j} \underline{\underline{I}} - \frac{\alpha_j}{\theta_j^2} \underline{\underline{A}}t - \frac{\alpha_j}{\theta_j^3} \underline{\underline{A}}^2 t^2 + O(t^3) \right) \right] \right\} \quad (20)$$

We now collect powers of $\underline{\underline{A}}t$:

$$\begin{aligned} n = 0 : \alpha_0 - 2\text{Re} \left[\sum_{j=1}^{k/2} \frac{\alpha_j}{\theta_j} \right] \\ n > 0 : -2\text{Re} \left[\sum_{j=1}^{k/2} \frac{\alpha_j}{\theta_j^{n+1}} \right]. \end{aligned} \quad (21)$$

Now we need to require that these expressions match the power series terms found in Eq. 18 to guarantee a certain order of accuracy. If the first term $n = 0$ does not match Eq. 18's counterpart, CRAM is inconsistent. The following conditions are derived for the coefficients α_j and θ_j :

$$\begin{aligned} n = 0 : \alpha_0 - 2\text{Re} \left[\sum_{j=1}^{k/2} \frac{\alpha_j}{\theta_j} \right] &= 1 \\ n > 0 : -2\text{Re} \left[\sum_{j=1}^{k/2} \frac{\alpha_j}{\theta_j^{n+1}} \right] &= \frac{1}{n!}. \end{aligned} \quad (22)$$

Table 1: Relative difference between right and left hand side of the conditions layed out in Eq. 22 for different CRAM orders.

n	Cram order						
	4	6	8	10	12	14	16
0	-8.65E-05	-1.01E-06	-1.17E-08	-1.36E-10	-1.60E-12	-1.73E-14	-6.33E-15
1	-3.13E-03	-5.26E-05	-7.98E-07	-1.14E-08	-1.58E-10	-2.13E-12	-3.30E-14
2	-3.80E-02	-9.17E-04	-1.82E-05	-3.21E-07	-5.28E-09	-8.23E-11	-1.24E-12
3	-2.84E-01	-9.71E-03	-2.50E-04	-5.43E-06	-1.06E-07	-1.92E-09	-3.27E-11
4	-1.57E+00	-7.50E-02	-2.48E-03	-6.62E-05	-1.53E-06	-3.20E-08	-6.21E-10
5	-7.02E+00	-4.63E-01	-1.95E-02	-6.34E-04	-1.73E-05	-4.18E-07	-9.20E-09
6	-2.61E+01	-2.41E+00	-1.28E-01	-5.04E-03	-1.62E-04	-4.51E-06	-1.12E-07
7	-7.73E+01	-1.10E+01	-7.27E-01	-3.44E-02	-1.30E-03	-4.14E-05	-1.17E-06
8	-1.27E+02	-4.49E+01	-3.67E+00	-2.08E-01	-9.13E-03	-3.34E-04	-1.06E-05

The the coefficients used are given in [9] that are also used in the Serpent code. The relative difference of the right and left hand side of Eq. 22 are presented in Table 1 for CRAM orders 2, 4, 6, 8, 10, 12, 14, and 16 and for terms $n = 0, \dots, 8$. First it should be pointed out that there is a limit of the number of terms CRAM can satisfy before running out of degrees of freedom (i.e. the coefficients) to satisfy them. CRAM-4 comprises 9 coefficients (α_0 is real), so it is theoretically capable of satisfying conditions $n = 0$ to $n = 8$. However, the results in Table 1 indicate that

it does not exactly satisfy any condition, not even the condition for $n = 0$ which is required for consistency. The observed relative differences for CRAM-4 increase with increasing n . When increasing the CRAM order, the relative difference decreases for a fixed n , but none of the CRAM orders represents any term indexed by n exactly even though the $n = 0$ term is matched to almost machine precision by CRAM-16. Hence, we conclude that CRAM is inconsistent in the following sense: if the CRAM order is fixed and the time step is decreased, CRAM's solution does not converge to the exact solution of the depletion problem. However, with increasing the CRAM order, the conditions incorporated in Eq. 22 are satisfied more closely. For sufficient CRAM order, CRAM will appear consistent up to machine round-off which invalidates any numerical experiment seeking more accuracy.

If the norm of the burnup matrix times the time step is small, i.e. $\|\underline{A}t\| = |t|\|\underline{A}\| < \text{threshold} < 1$, it may be beneficial to modify the CRAM coefficients to satisfy the conditions Eq. 22 up to some n exactly. For this purpose an efficient method for computing the norm of \underline{A} must be available, and a robust method for setting the threshold must exist.

3 Test Problems

The test problems described in this section are used to verify the microscopic depletion implementation in MAMMOTH. The level of complexity of each exercise is increased at each step to provide a comprehensive approach to benchmarking the implementation in MAMMOTH. Two analytic solutions are included in sections 3.1 and 3.2 and a code-to-code comparison is introduced section 3.3. The results to these problems are provided in Section 4.

3.1 Thorium Series

The Thorium-232 decay series, shown in Figure 1 [10], provides a very good data set for benchmarking the decay of isotopes, since it includes a variety of half-lives from billions of years to 1E-7 seconds. An converged accelerated semi-analytical benchmark for this series is available [11], but some issues were encountered in the initial document, namely: 1) the inconsistency of the decay constants and the the solution provided, 2) the lack of correspondence between the isotope indexing and the isotope name, 3) the lack of correspondence between the branching ratios and the isotope name, and 4) the number of significant figures provided for the time variable in the solution. All issues were satisfactorily resolved.

These issues have been corrected and the benchmark dataset is provided in Tables 2 through 4. The solution provided in Table 4 was obtained with the Doubling algorithm [11] where the time steps are found adaptively with Richardson or Wynn-Epsilon extrapolation. These results were confirmed via a Transmutation Trajectory Analysis (TTA) solution.

Table 2: Decay constants for the Thorium Series (per day)

Isotope	Decay Constant
Th-232	1.351625E-13
Ra-228	3.302667E-04
Ac-228	2.661685d+00
Th-228	9.934261E-04
Ra-224	1.908497E-01
Rn-220	1.077121E+03
Po-216	4.130201E+05
Pb-212	1.563490E+00
Bi-212	1.648442E+01
Po-212	2.002940E+11
Tl-208	3.269348E+02

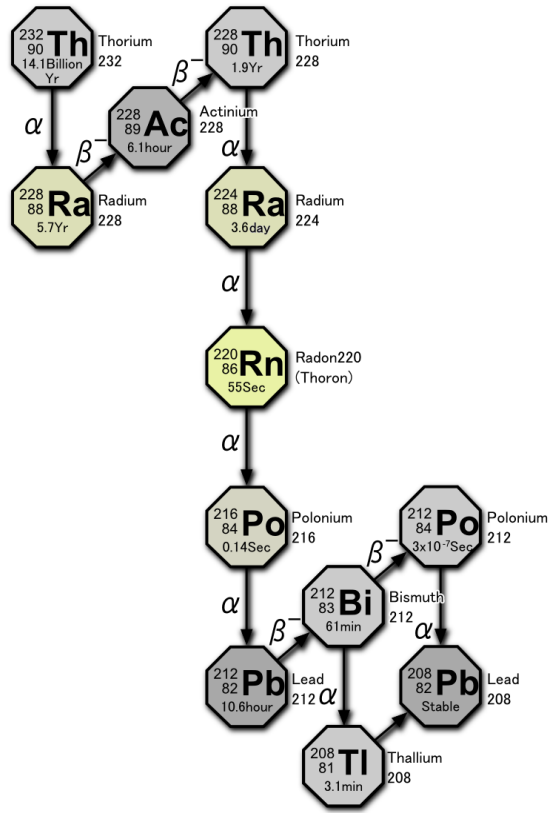


Figure 1: Thorium-232 decay series.

Table 3: Branching ratios for Bi-212

Daughter Isotope	Branching Ratio
Po-212	0.6406E+00
Tl-208	0.3594E+00

3.2 Constant Flux in a Homogeneous System

The next step is to check the CRAM solver against a constant flux analytic solution. For this, the simple U-235, I-135, and Xe-135 transmutation chain is employed. The analytic solution consists of a constant flux irradiation for 100 hrs followed by decay (zero flux) for another 100 hrs, as shown in Figure 2.

3.3 Code-to-Code Comparison to DRAGON5

Finally, a reference calculation is performed with DRAGON5 for an infinite homogeneous domain. The mixture is composed of homogenized PWR fuel and is depleted to 600 EFPD with a

Table 4: Reference solution for Thorium Series at 1 year. (1×10^{-12} relative error)

Time (days)	Th-232	Ra-228	Ac-228	Th-228	Ra-224	Rn-220
36.5	6.02299999970E+23	2.953567638154E+12	3.627339589142E+08	1.726783939692E+10	6.770295695164E+07	1.199525306804E+04
73.0	6.022999999941E+23	5.871744543953E+12	7.248715742555E+08	6.867693005511E+10	3.102328977782E+08	5.496713712636E+04
109.5	6.022999999911E+23	8.754954782151E+12	1.082669923668E+09	1.525986405848E+11	7.231989443712E+08	1.281377826921E+05
146.0	6.02299999881E+23	1.160361733620E+13	1.436181001830E+09	2.674636649886E+11	1.298389797172E+09	2.300522691959E+05
182.5	6.02299999851E+23	1.441814616915E+13	1.785456180401E+09	4.117635120055E+11	2.027908498993E+09	3.593113727562E+05
219.0	6.02299999822E+23	1.719895028378E+13	2.130546215485E+09	5.840482803810E+11	2.904164707130E+09	5.145701970348E+05
255.5	6.02299999792E+23	1.994643378205E+13	2.471501255008E+09	7.829245140706E+11	3.919863473831E+09	6.945361853018E+05
292.0	6.02299999762E+23	2.266099592383E+13	2.808370846007E+09	1.007053134518E+12	5.067994426381E+09	8.97967203074E+05
328.5	6.02299999733E+23	2.534303118491E+13	3.141203941827E+09	1.255147447262E+12	6.341821336098E+09	1.123669691062E+06
365.0	6.02299999703E+23	2.799292931431E+13	3.470048909235E+09	1.525971220201E+12	7.734872062336E+09	1.370496881064E+06

Time (days)	Po-216	Pb-212	Bi-212	Po-212	Tl-208	Pb-208
36.5	3.128258654688E+01	7.939993206442E+06	7.501737681487E+05	3.955073325537E-05	1.359150693723E+04	1.310116157156E+08
73.0	1.433495695291E+02	3.717037958899E+07	3.519211116439E+06	1.855401855481E-04	6.376713399337E+04	1.313896772178E+09
109.5	3.341723329185E+02	8.722319214702E+07	8.263344020327E+06	4.356608148962E-04	1.497343094422E+05	4.761869212390E+09
146.0	5.999565686358E+02	1.570954782267E+08	1.488744026561E+07	7.848970515905E-04	2.697691038058E+05	1.163451205090E+10
182.5	9.370532207864E+02	2.458226146684E+08	2.330000268061E+07	1.228424972983E-03	4.222134591463E+05	2.303525827430E+10
219.0	1.341954915050E+03	3.524774300961E+08	3.341308648481E+07	1.761607945931E-03	6.054736918563E+05	4.001356399748E+10
255.5	1.811290774316E+03	4.761688345707E+08	4.514216930889E+07	2.379989773984E-03	8.180181372398E+05	6.356700654227E+10
292.0	2.341821418979E+03	6.160404979930E+08	5.840602583819E+07	3.079288088324E-03	1.058374877876E+06	9.464330569818E+10
328.5	2.930434146939E+03	7.712695760090E+08	7.312660696192E+07	3.855387976254E-03	1.325129553631E+06	1.341422709222E+11
365.0	3.574138286889E+03	9.410654817207E+08	8.922892326710E+07	4.704335838763E-03	1.616923250406E+06	1.829176771398E+11

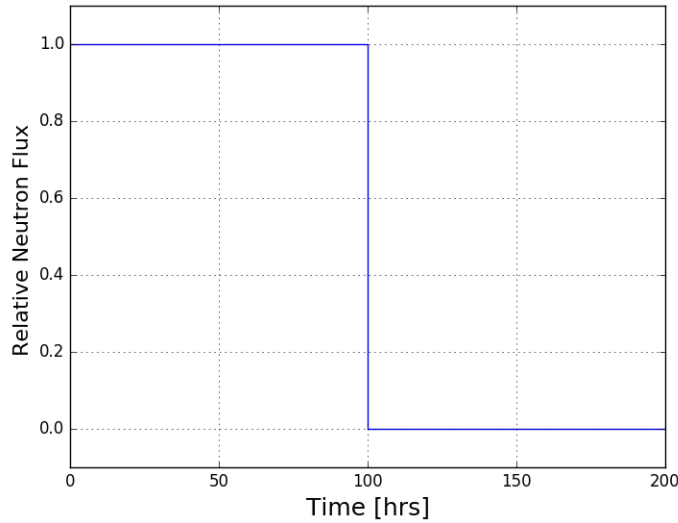


Figure 2: Irradiation history for constant flux test.

fixed power level. The DRAGON5 depletion calculations are conducted on a much finer time discretization than the MAMMOTH calculation and employ a fifth order Cash-Karp algorithm for the time integration. The matrix multiplications and linear system solutions are obtained via the LU decomposition. No equilibrium assumption is used for the fission products during this calculation.

The 361 group flux solution from DRAGON5 is used in the generation of the energy-collapsed (one-group) neutron cross sections. The decay and transmutation data used in MAMMOTH is based on the DRAGON5 dataset, which is itself derived from ENDF/B-VII.r1 data. The DRAGON5 dataset includes 297 nuclides and was converted to the XML standard used in MAMMOTH.

MAMMOTH uses Rattlesnake to perform eigenvalue calculations, although the solution is trivial in this test, with the macroscopic cross sections based on the time evolution of the isotopic composition. The Rattlesnake fluxes are not used in the depletion in order to avoid differences in the power normalization between MAMMOTH and DRAGON5. Instead, one-group fluxes from the DRAGON5 calculation are used in MAMMOTH to perform the depletion calculation.

4 Results

The results to the test problems introduced in Section 3 are discussed in this section and follow the same order. The results include testing of the CRAM order and time convergence.

4.1 Thorium Series

The relative error at 1 year for a number of nuclides using the CRAM solver as a function of polynomial order is included in Figure 3. These solutions were obtained from a single 1 year step. As the polynomial order is increased the solution quickly approaches the precision of the reference calculation.

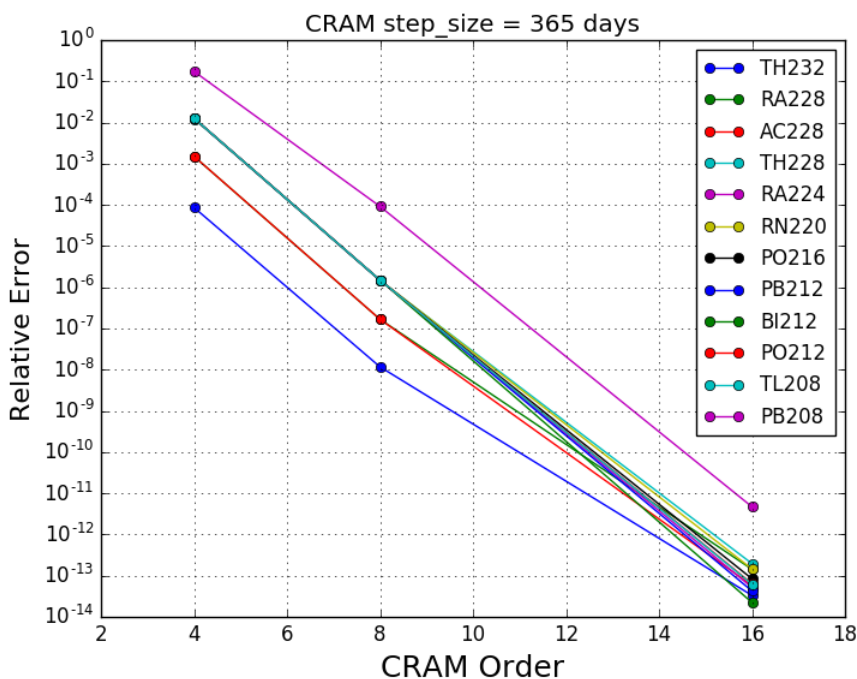


Figure 3: CRAM order convergence for the Thorium chain.

The time evolution of the relative error for orders 8 and 16 is included in Figure 4. The maximum relative error with the 8th order solution is near 4×10^{-4} , whereas with order 16, the solution remains within the precision of the reference calculation.

The Thorium benchmark reference results were extended to 100 billion years in order to test the accuracy of the solver with very large time steps. The order 16 CRAM is exclusively used for this particular problem and it shows little sensitivity to the time step size. Figure 5 shows the absolute relative errors for very large time step sizes of 100 million and 1 billion years. In addition, a

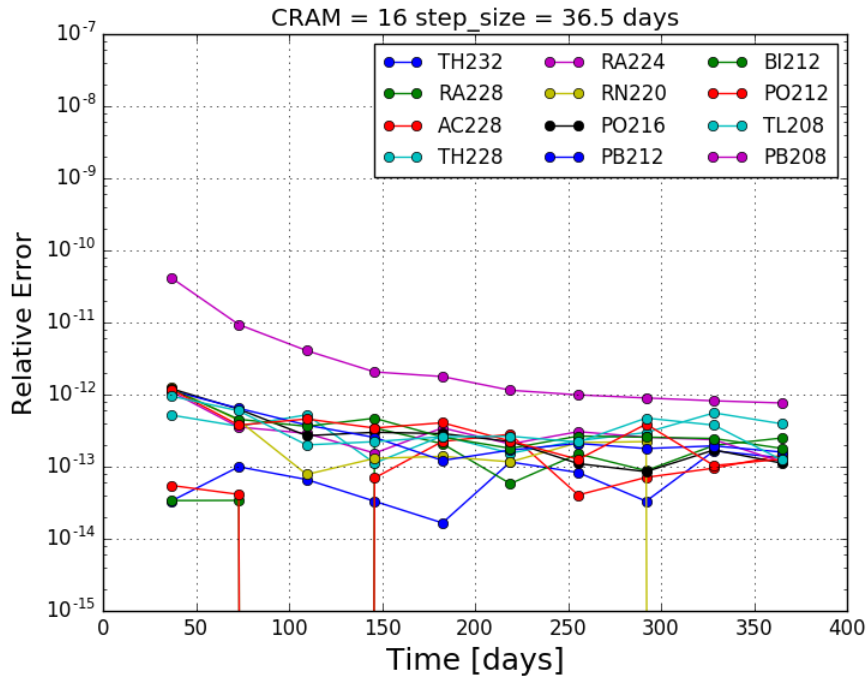
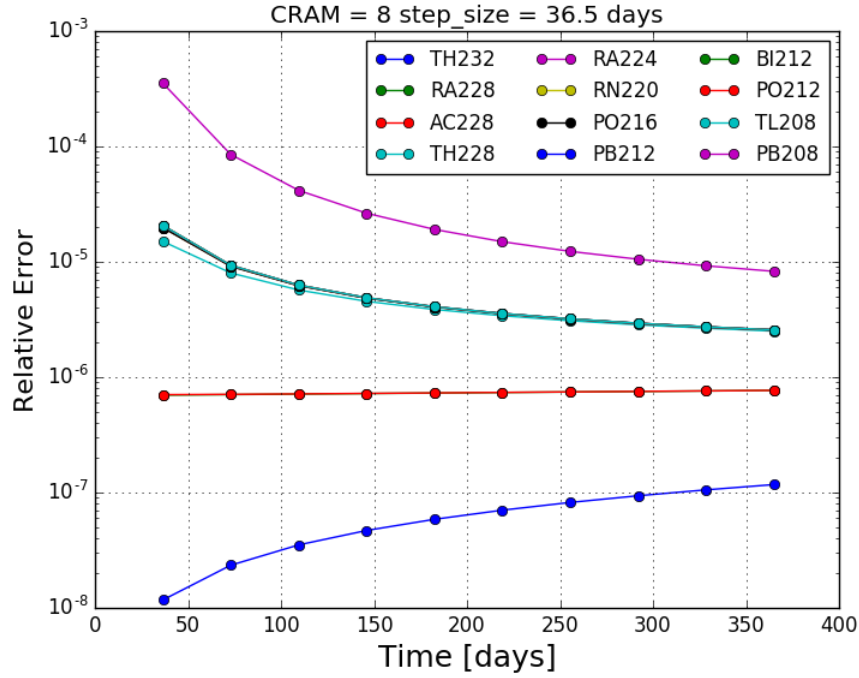


Figure 4: Relative error of the MAMMOTH Thorium chain solution at 1 year. (Benchmark accuracy $\sim 1 \times 10^{-12}$ relative error)

single 100 billion year step was tested and the results remain within the accuracy of the reference calculation.

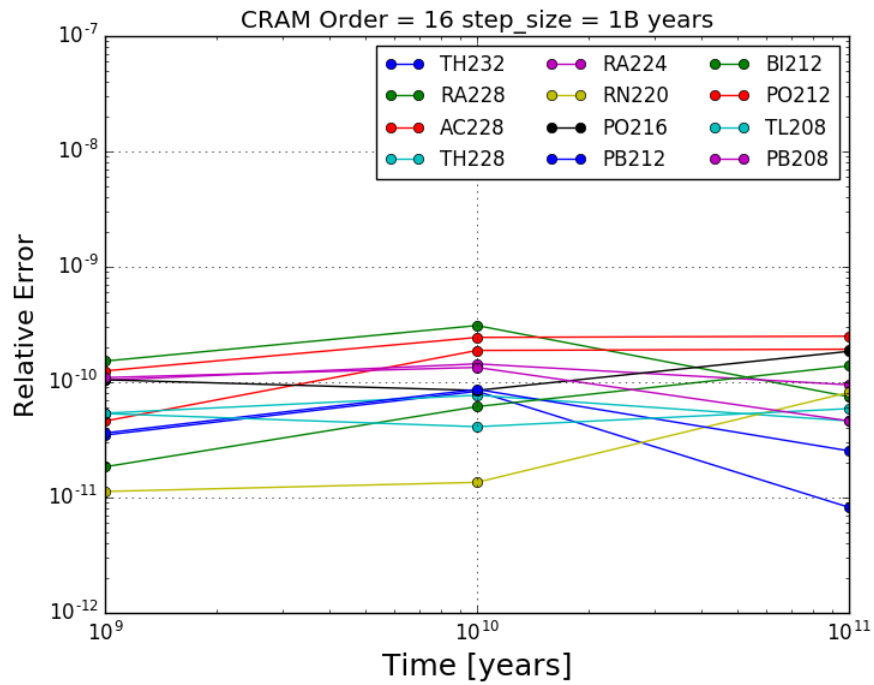
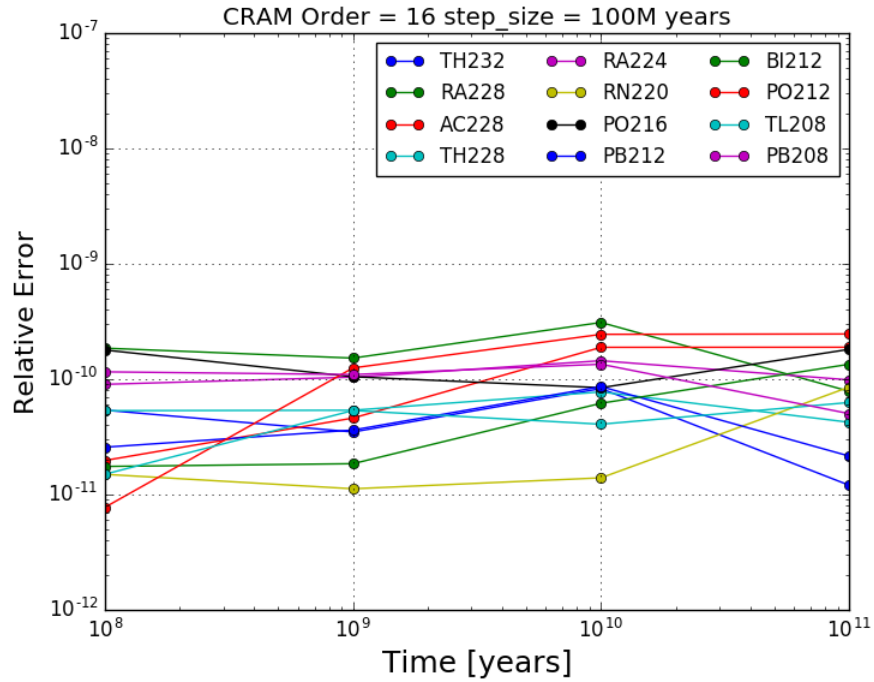


Figure 5: Relative error of the MAMMOTH Thorium chain solution at 100 billion years. (Benchmark accuracy $\sim 1 \times 10^{-9}$ relative error)

4.2 Constant Flux in a Homogeneous System

Both the analytic and the MAMMOTH solutions for the U-235, I-135 and Xe-135 transmutation chain test are shown in Figure 6. The I-135 and Xe-135 concentrations reach the saturation point during the constant flux depletion. At 100 hrs the flux level is decreased to 0 and the I-135 continues to decay into Xe-135, thus creating a typical Xe transient event.

A CRAM order test is included in Figure 7. The relative errors with order 8 remain below 2×10^{-6} . With CRAM order 16, even though it appears to degrade over time, the solution remains within the precision of the reference calculation, below 1×10^{-12} . Since the flux level changes twice during the problem, two time steps are the minimum required to capture the two different flux levels with the CRAM solver. The relative error of CRAM order 16 with two-100 hour steps is shown in Figure 8 and remains within the precision of the reference.

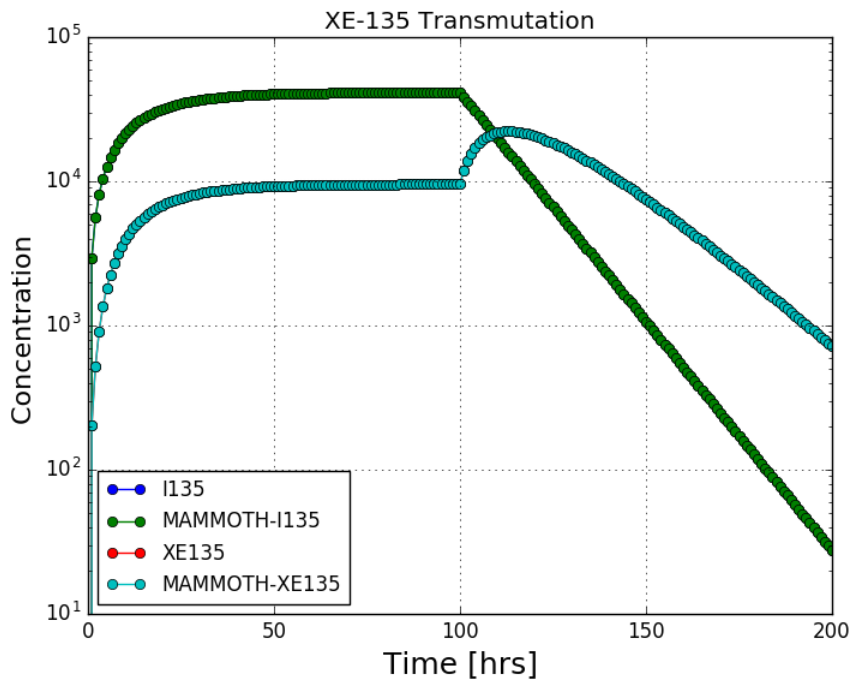


Figure 6: Reference and MAMMOTH solution for the Xe-135 chain.

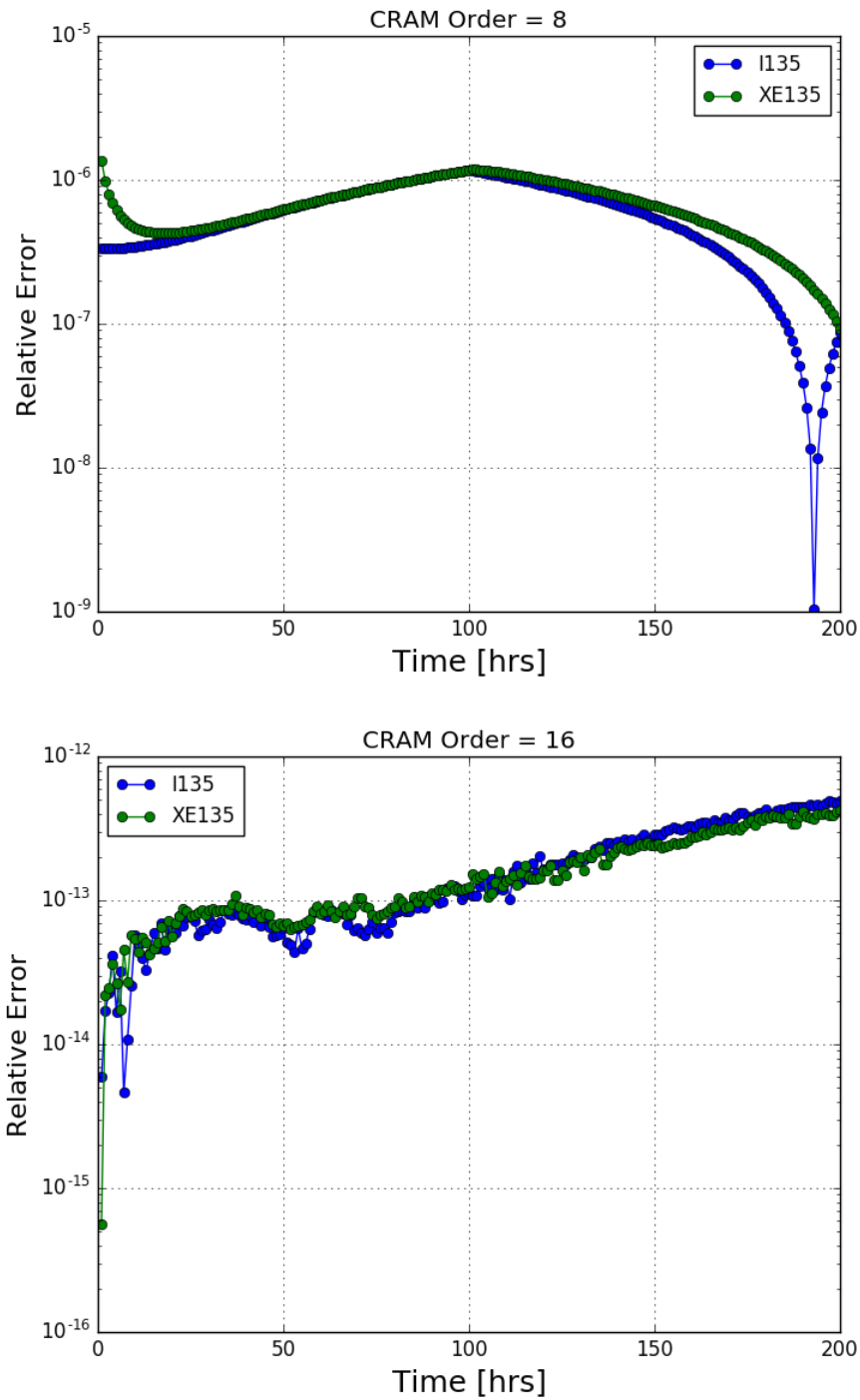


Figure 7: CRAM order convergence for the Xe-135 chain (1 hr time step). (Benchmark accuracy $\sim 1 \times 10^{-12}$ relative error)

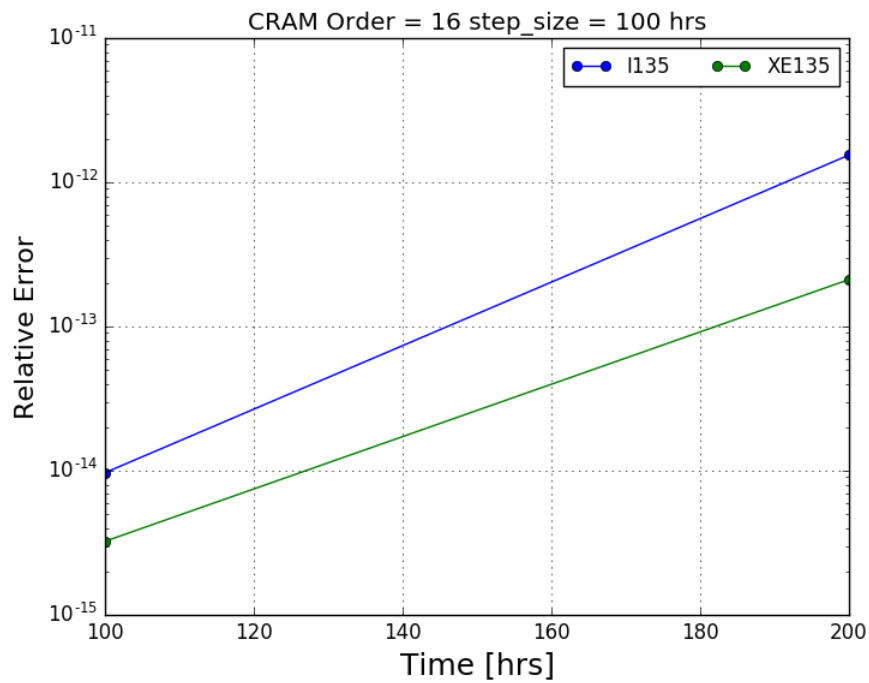


Figure 8: Relative error for the Xe-135 chain with large time steps. (Benchmark accuracy $\sim 1 \times 10^{-12}$ relative error)

4.3 Code-to-Code Comparison to DRAGON5

The reactivity curve for the infinite homogeneous domain depletion up to 600 EFPD is shown in Figure 9. The difference between the MAMMOTH and the DRAGON5 reference solution remains within 20 pcm using CRAM order 16. This result indicates that there is a discrepancy in the depletion of the fuel, since, with the direct use of the DRAGON5 fluxes, the difference is expected to remain within a few pcm of the reference. The DRAGON5 solution is well converged and differences arising from the solution method for the burnup equations can be disregarded, considering that the DRAGON5 solution uses a much finer temporal discretization with a 5th order time integration method. Therefore, the differences cannot be attributed to the solution method and probably arise from discrepancies in the data.

Analysis of the isotopic data for a few actinides, shown in Figures 10 to ,12 demonstrates that the depletion of U-235 degrades steadily up to 0.4% of the reference at 600 EFPD. The Pu-239 concentration is also over-predicted by almost 1.40% and indicates a potential problem with the capture and fission reactions. Pu-240 is produced via capture of Pu-239, thus shows the compounded error of 2.3%. Some fission products are included in Figures 13 to 15. Of particular interest is I-135, which shows a fluctuation in the saturation point at 50 EFPD. This is long past the 50 hr point for the saturation of this isotope. In addition, a peak error of 2.3% is observed near 75 EFPD. The Xe-135 concentration does not show this effect and the relative difference remains below 0.5%. Sm-149, which is stable and can only be removed by neutron capture, shows a similar peak in the error at the same 75 EFPD point, which coincidentally matches the peak error in Pu-240. In order to resolve these differences, a detailed examination of the DRAGON5 and the MAMMOTH exponential matrix is necessary and will be conducted in future work.

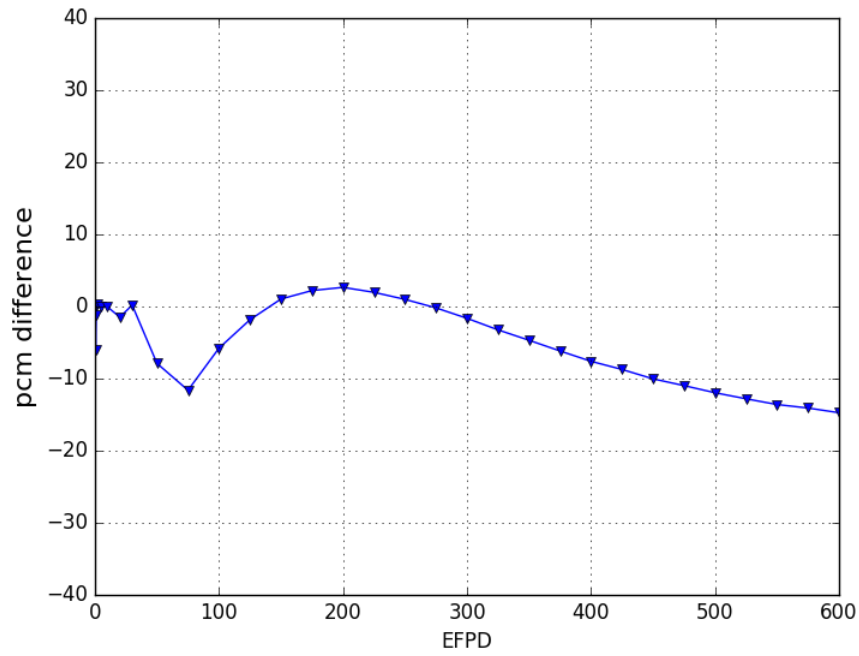
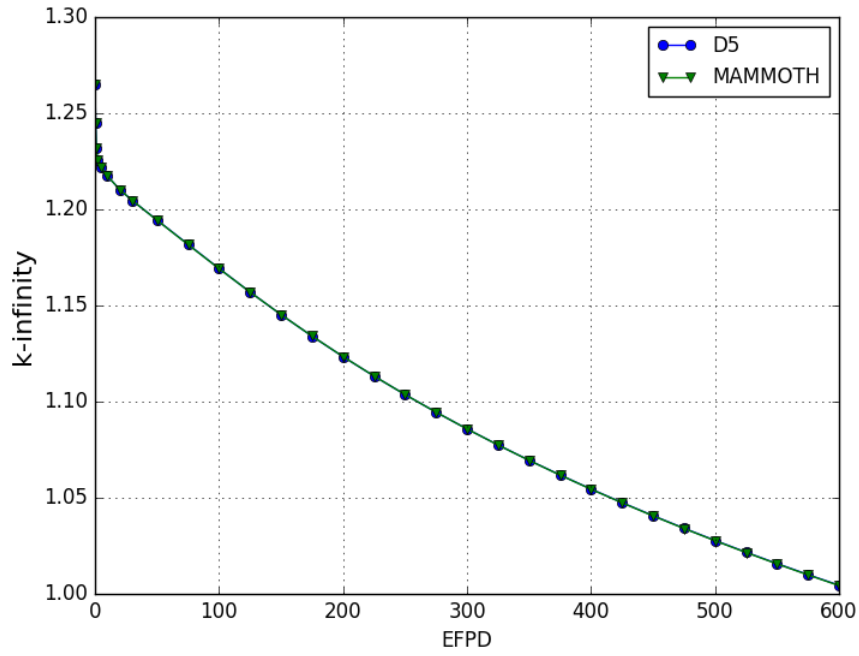


Figure 9: Reactivity curve for the homogeneous infinite domain problem.

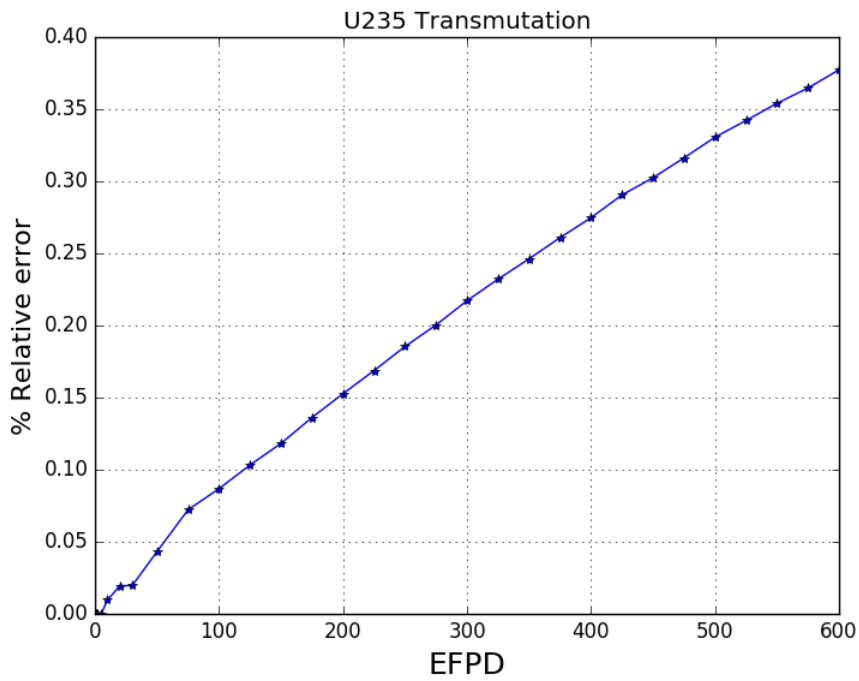
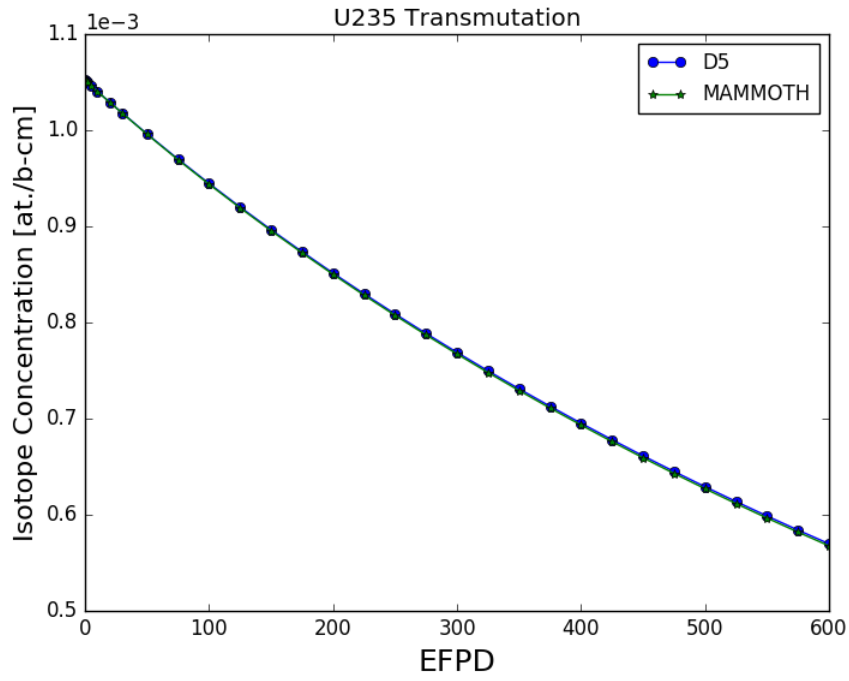


Figure 10: Isotopic concentrations and relative differences for U235.

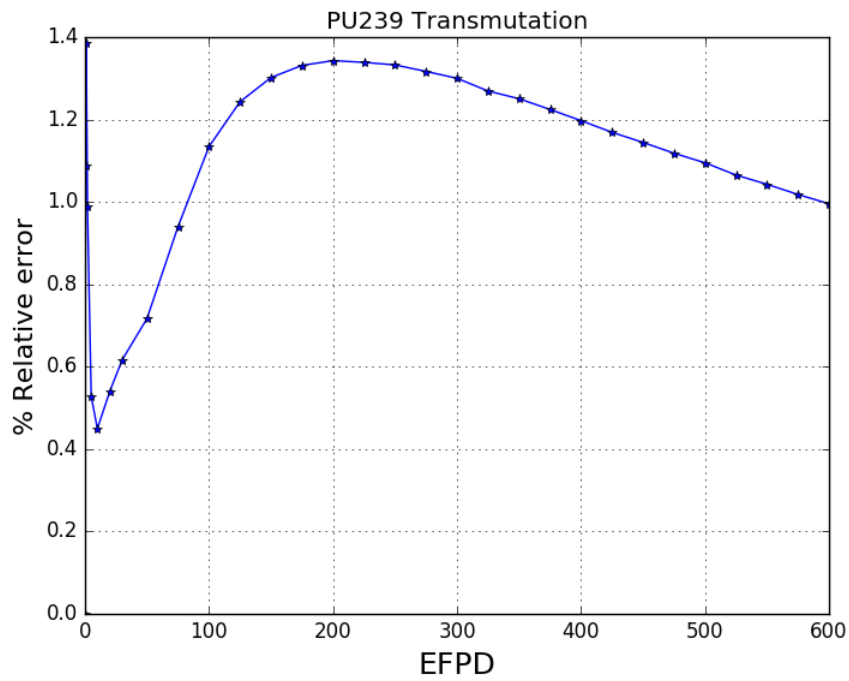
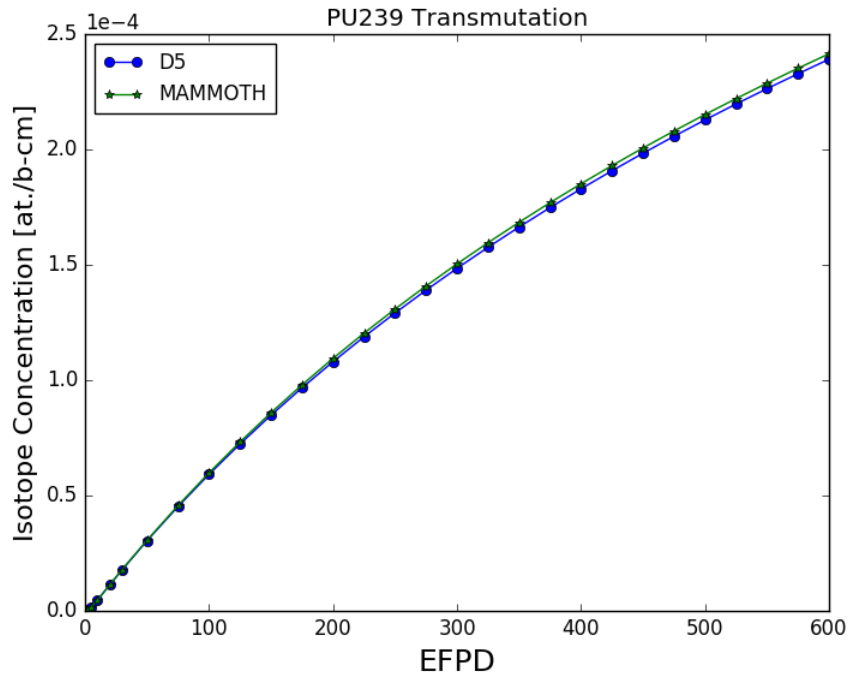


Figure 11: Isotopic concentrations and relative differences for Pu239.

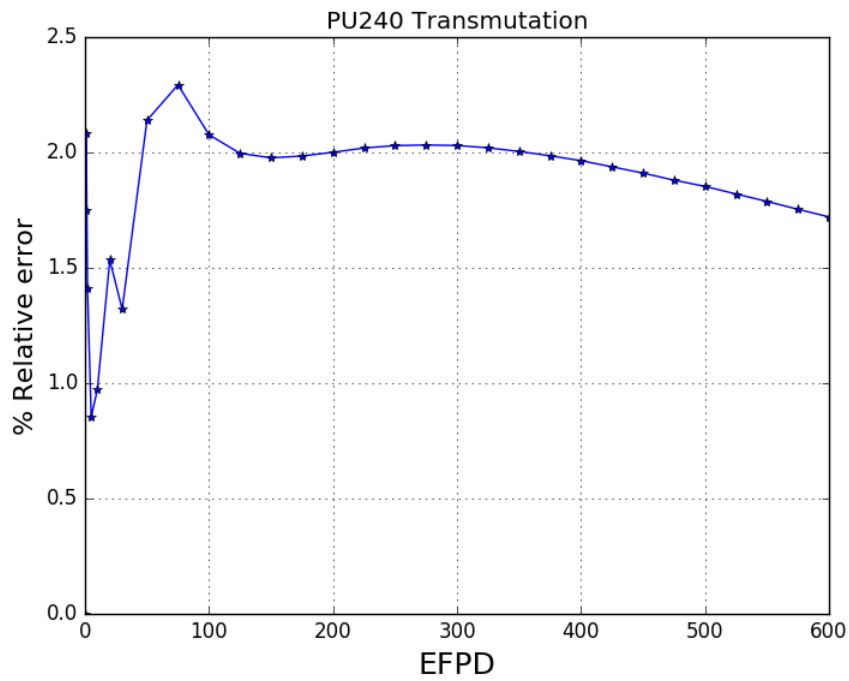
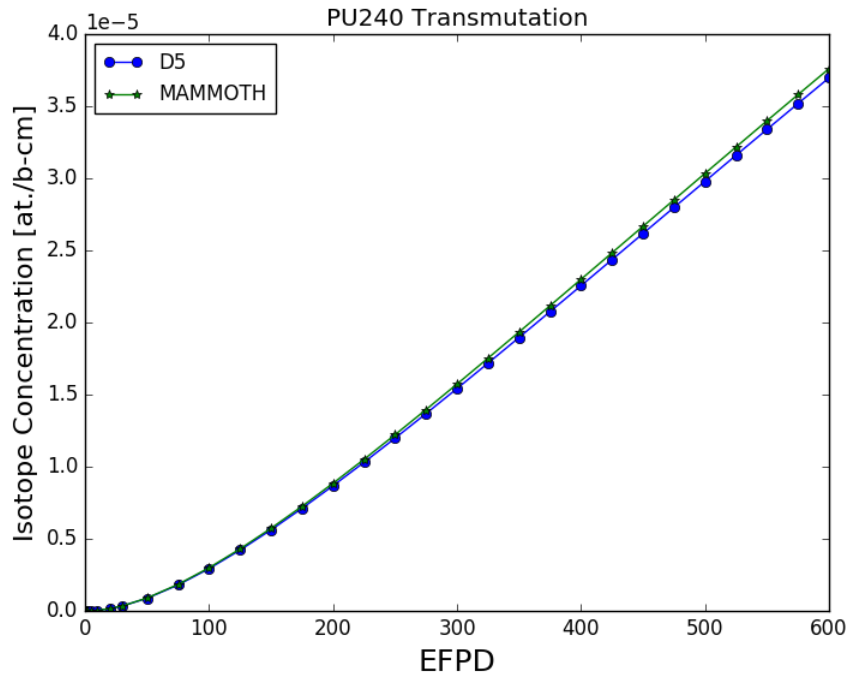


Figure 12: Isotopic concentrations and relative differences for Pu240.

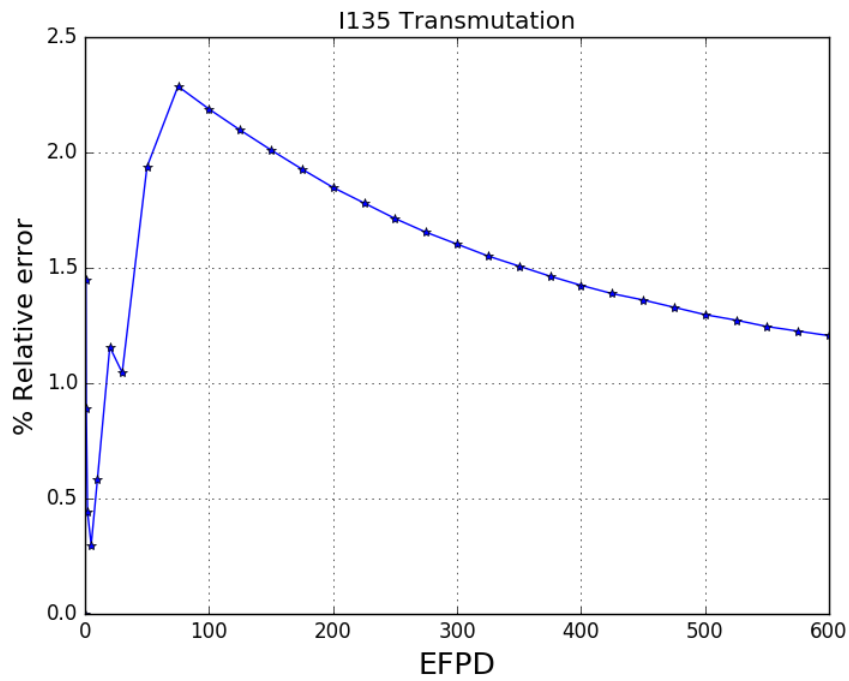
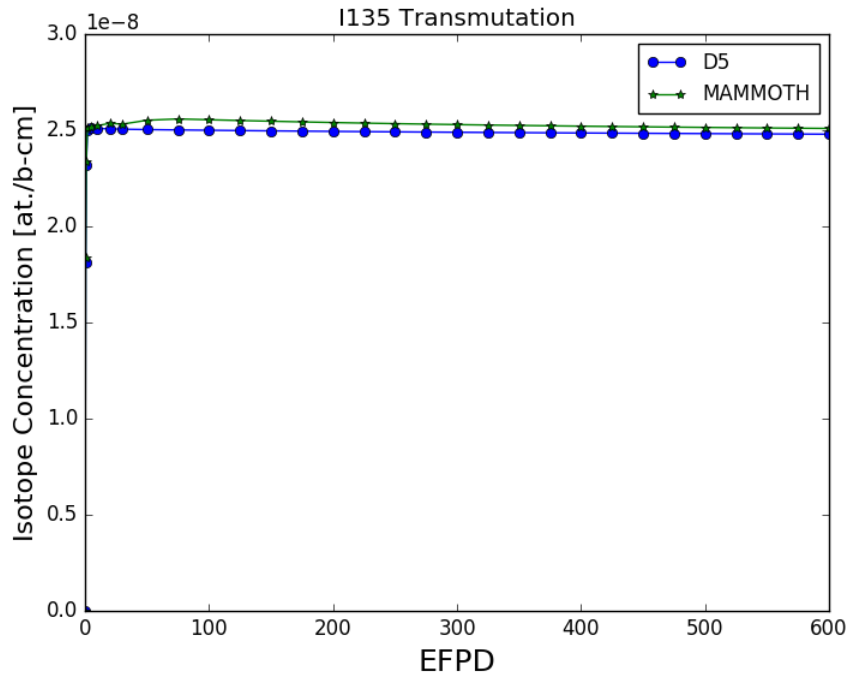


Figure 13: Isotopic concentrations and relative differences for I135.

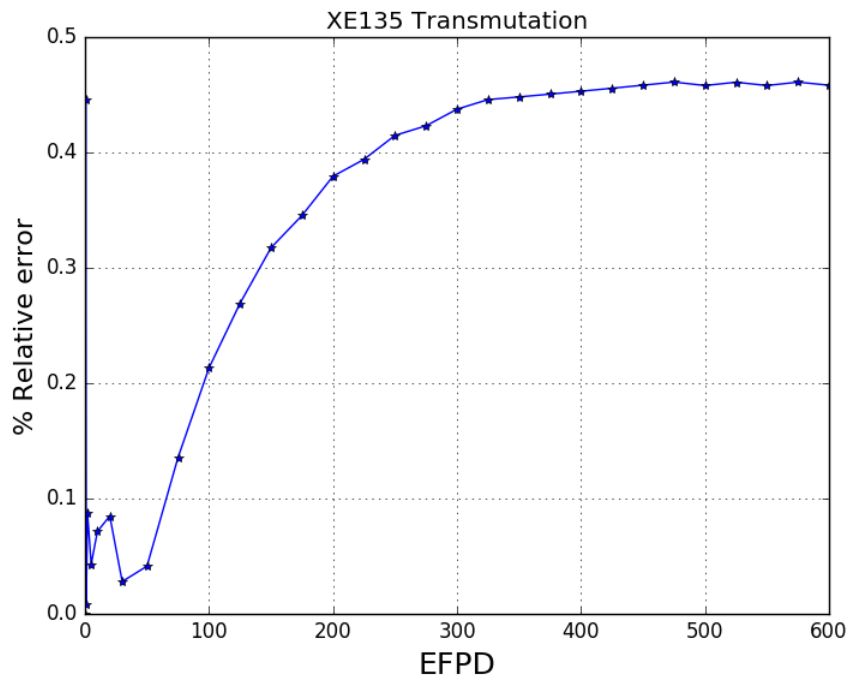
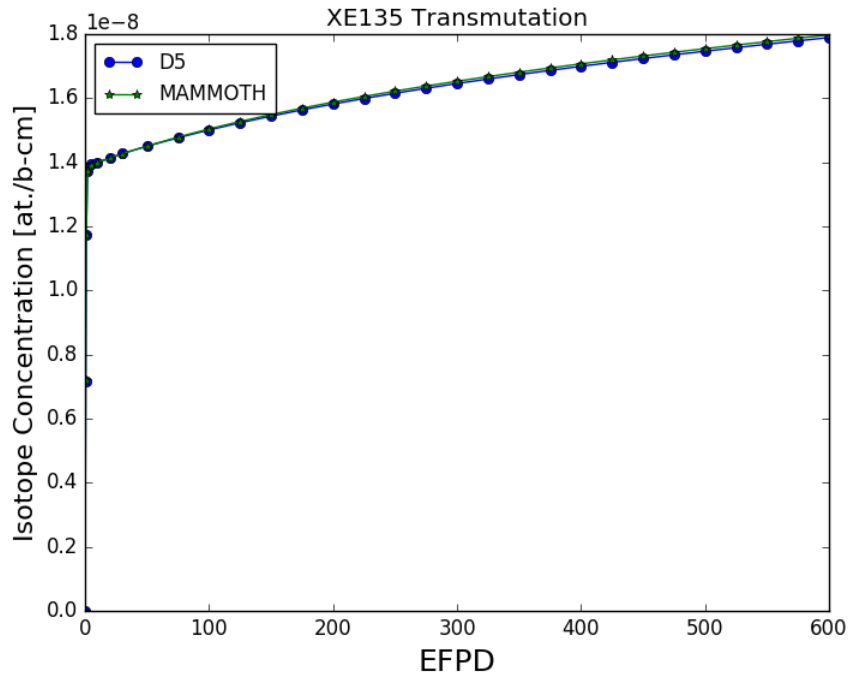


Figure 14: Isotopic concentrations and relative differences for XE135.

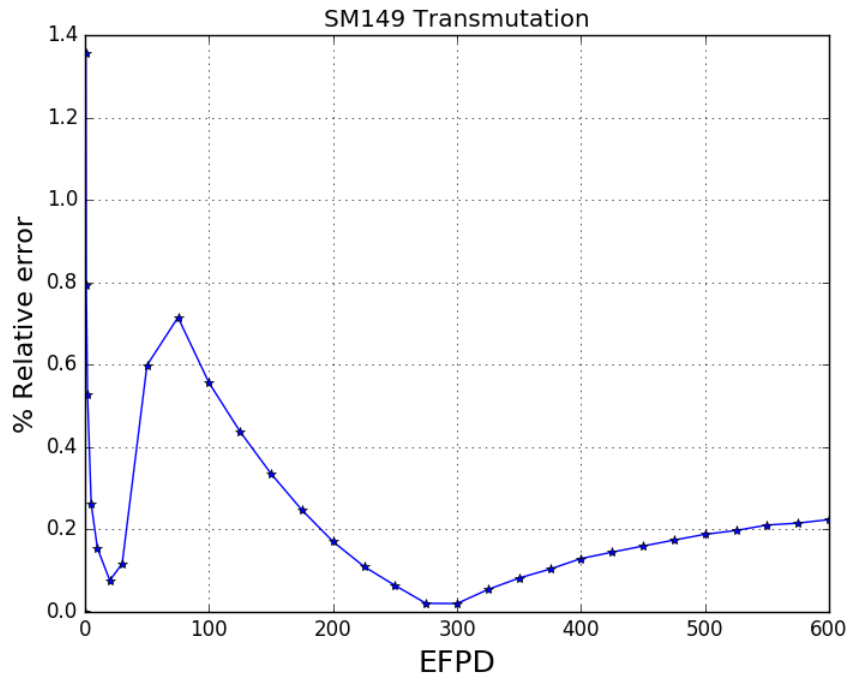
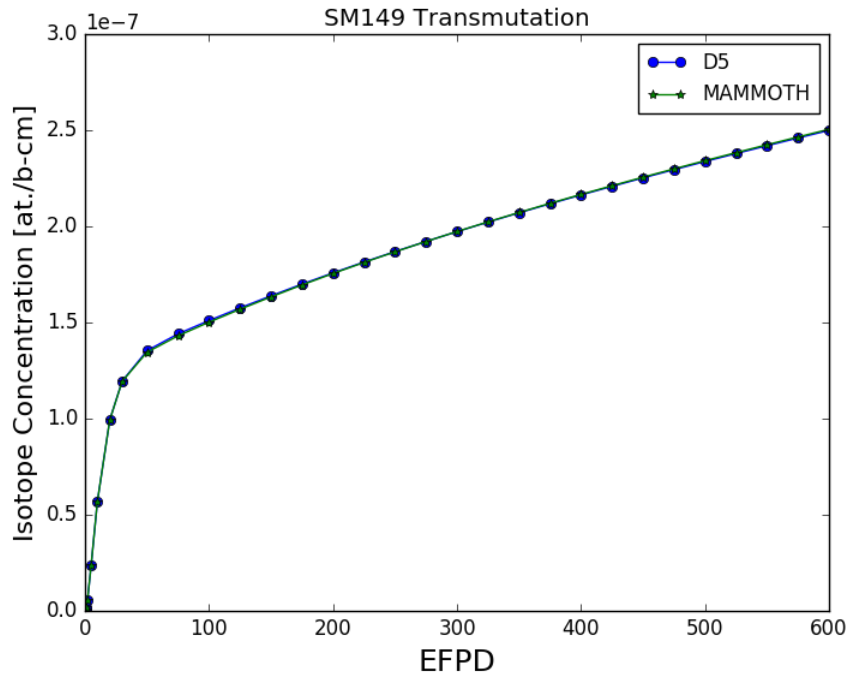


Figure 15: Isotopic concentrations and relative differences for SM149.

5 Conclusions and Future Work

This report shows that the implementation of the CRAM solver within MAMMOTH is correct and it matches various analytic benchmarks for decay and transmutation of nuclides within the level of accuracy of the benchmark. The 16th order CRAM solutions show little sensitivity to the time step size, achieving a high level of accuracy for isotopic decay for time steps of 100 billion years. A few problems were encountered with data inconsistencies in the comparison to DRAGON5, but the differences in the reactivity curve throughout the 600 EFPD depletion remain within 20 pcm of the reference. The isotopic distributions show differences that require further analysis.

Future work includes:

- the continued collaboration with the University of Arizona to generate a larger reference benchmark for the depletion of 297 isotopes at a constant flux,
- the detailed examination of the DRAGON5 and the MAMMOTH exponential matrix coefficients to resolve current differences,
- the depletion of an infinite domain at a fixed power level with multiple energy groups,
- the depletion of a heterogeneous fuel cell at a constant flux with multiple energy groups,
- the depletion of a heterogeneous fuel cell at a fixed power level with multiple energy groups,
- the improvement to the decay and transmutation dataset by extending the number of isotopes,
- correcting the implementation of the IPF method and conducting the same test suite,
- and the performance of multiple validation studies against measurements.

References

- [1] F. N. Gleicher, J. Ortensi, et. al. The Coupling of the Neutron Transport Application Rattlesnake to the Fuels Performance Application BISON. In *International Conference on Reactor Physics (PHYSOR 2014)*, Kyoto, Japan, May 2014.
- [2] Derek Gaston, Chris Newman, Glen Hansen, and Damien Lebrun-Grandie. MOOSE: A Parallel Computational Framework for Coupled Systems of Nonlinear Equations. *Nuclear Engineering and Design*, 239(10):1768–1778, 2009.
- [3] R.L. Williamson et al. Multidimensional Multi-physics Simulation of Nuclear Fuel Behavior. *Jou. Nucl. Mat.*, 423(149–163), 2012.
- [4] D. Andrs et al. Relap-7 Level 2 Milestone Report: Demonstration of a Steady State Single Phase PWR Simulation with RELAP-7. Technical Report INL/EXT-12-25924, Idaho National Laboratory, 2012.
- [5] Yaqi Wang. Nonlinear Diffusion Acceleration for the Multigroup Transport Equation Discretized with SN and Continuous FEM with Rattlesnake. In *Proceedings to the International Conference on Mathematics, Computational Methods & Reactor Physics (M&C 2013)*, Sun Valley, Idaho, USA, May 5-9 2013.
- [6] F. Gleicher and J. Ortensi et al. The Application of MAMMOTH for a Detailed Strongly Coupled Fuel Pin Simulation with a Station Blackout. American Nuclear Society, 2016.
- [7] H. Bateman. The Solution of a System of Differential Equations Occurring in the Theory of Radioactive Transformations. In *Proceedings of the Cambridge Philosophical Society, Mathematical and physical sciences*, volume 15, pages 423–427. University Press, 1910.
- [8] Maria Pusa. Higher Order Chebyshev Rational Approximation Method and Application to Burnup Equations. *Nuclear Science and Engineering*, 182:297–318, 2016.
- [9] Maria Pusa. Rational approximations to the matrix exponential in burnup calculations. *Nuclear Science and Engineering*, 169(2):155167, 2011.
- [10] Tosaka. Decay Chain 4n, Thorium Series. <http://www.commons.wikimedia.org>, 2010 (accessed December 7, 2014).
- [11] K. Huang, Y. Li, and B. Ganapol. A Backward Euler Doubling Feasibility Study Based on Thorium Series Cascade. In *Transactions of the American Nuclear Society*, volume 114, pages 399–402. American Nuclear Society, 2016.
- [12] J. Leppänen. Development of a New Monte Carlo Reactor Physics Code. D.Sc. Thesis VTT Publications 640, Helsinki University of Technology, 2007.
- [13] G. Marleau, A. Hébert, and R. Roy. A User Guide for Dragon Version5. IGE-335, École Polytechnique de Montréal, March 2016.
- [14] Alain Hebert. *Applied Reactor Physics*. Presses Internationales Polytechnique, 2009.

- [15] Maria Pusa and Jaakko Leppanen. Computing the matrix exponential in burnup calculations. *Nuclear Science and Engineering*, 164(1):140150, 2009.

